Heritage Science

RESEARCH

Open Access

Atmospheric corrosion in the metal pool of Ali Qapu palace in Isfahan: an experimental study

Mehri Raoufifar[1] and Omid Oudbashi[1,2*]

Abstract

Isfahan, the capital of Iran during the Safavid period (1501–1736 CE), houses the Ali Qapu Palace. It was constructed during the Safavid period to be used as the royal court and a place for settling the affairs of the country. The palace was built in five stages; the final stage was the porch which contains a pool at its centre. The perimeter of the pool is made of white marble, the floor and walls are covered with metal sheets to which the marble is attached. Today, the dry pool is exposed to the urban environment of the metropolis of Isfahan. This study investigates the composition and the corrosion mechanism of the pool using optical microscopy, ICP-OES, SEM–EDS and X-ray diffraction techniques. The results show that the pool's cover is made of a large number of sheets of copper joined together by copper and lead nails. The forging (cold-working and annealing) method was used to form the sheets. The corrosion products formed on the surface of the copper sheets are copper oxide and copper trihydroxychlorides. The mechanism of corrosion in the metal pool, including copper oxidation, is due to the formation of copper (II) compounds resulting from the reaction with Cl-contaminated airborne particulate matters (dust).

Keywords Ali Qapu palace, Metal pool, Copper, Atmospheric corrosion, Urban environment, Air pollutants

Introduction

Atmospheric corrosion may cause the serious deterioration of historical metal artefacts and monuments. Analysing the corrosion products, providing the authenticity of the object and the corrosion factors that have changed its condition, can be helpful in decision making [1]. Hence, identifying and controlling the environmental conditions which result in corrosion is crucial. The rate of corrosion is affected by various factors including relative humidity (RH), particulate matter (PM) and gaseous pollutants such as sulphur dioxide and carbon dioxide, which significantly accelerate corrosion [1, 2]. When an artefact is exposed to the atmosphere, depending on the environment, several layers of corrosion products may form across the surface [1, 3]. This process may have a destructive impact on the surface of the artefacts. Hence, there is a need to take comprehensive action to protect artefacts as part of our cultural heritage [4–6]. While the corrosion and conservation of cultural heritage metalworks in atmospheric environments has been well studied in many countries (e.g., [7–12]), scant research has been conducted in this field in Iran [13]. Considerable worldwide research has focused on the corrosion and conservation of copper and its alloys (particularly tin bronze and brass):

A) Laboratory studies that determine the mechanism and morphology of corrosion in urban, rural, and marine environments (e.g., [13–21]);

*Correspondence:
Omid Oudbashi
o.oudbashi@aui.ac.ir; Omid.Oudbashi@metmuseum.org
[1] Department of Conservation of Cultural and Historical Properties, Art University of Isfahan, Hakim Nezami Street, Sangtarashha Alley, P.O.Box: 1744, Isfahan, Iran
[2] Department of Scientific Research, The Metropolitan Museum of Art, 1000 5th Avenue, New York 10028, USA

B) Studies that evaluate and estimate the corrosion reactions and rate of copper alloys in simulated conditions (e.g., [22–24]);
C) Studies that apply novel analytical methods to the study of atmospheric corrosion and conservation (e.g., [25–28]);

The aim of this study is to understand the corrosion mechanism and conditions required to conserve the Ali Qapu metal pool and to provide guidelines to the conservators who will implement an effective conservation strategy.

Historical background

Isfahan became the capital of Persia (Iran) for the second time in its history during the Safavid dynasty, which ruled Iran for 235 years (907–1148 AH/1501–1736 CE) [29]. The Ali Qapu Palace, which is now an important historical monument, is located in the Naqsh-e Jahan Square World Heritage Site in Isfahan [29, 30]. The historical monuments of Naqsh-e Jahan Square, including the Ali Qapu Palace, were constructed between 1598 and 1629 CE by Shah Abbas I and the other Safavid kings. It was the tallest habitable building of the Safavid dynasty, and the roof of the palace offers a panoramic view of the city. The construction of the Naqsh-e Jahan Square took place over several decades and during the reign of several important Safavid kings [31]. The palace is located at the west side of Naqsh-e Jahan Square, in front of Sheikh Lotfollah Mosque (Fig. 1a). The palace is about forty-eight metres high and comprises six floors. This building was constructed in five stages, where a section was added in each stage to make it look modern (Fig. 1b). The entrance was built first, the second stage expanded the building's footprint, the third stage was the last floor construction, followed by the east ledge, and the final stage was to cover the hall and the southern staircase.

A few further floors were added to the building over time, mainly during the reign of Shah Abbas I. Later, during the reign of Shah Abbas II, a columned porch was added to the east side of the residential rooms, and it was constructed over a span of 70 years. This large porch has eighteen wooden columns founded on stone bases. It is covered with a wooden ceiling which is decorated with paintings. In the middle of this porch, there is a beautiful marble pool, which has eight sides, and its surface is covered with numerous metal sheets as the floor of the pool [31–33].

This study focuses on the rectangular-shaped metal pool (6.6 m in length; 4.33 m wide and the depth of the pool is 0.38 m) which is bevelled in one corner (Figs. 1c, 2 and 3). The pool is not in use now and is empty for many years. It has been constructed and added to the porch at the Safavid period. The pool is surrounded by marble blocks and the floor of the pool is made of 76 small and large metal sheets which are either rectangular or circular. The walls of the pool are made of rectangular sheets which are not uniform in size and are joined together with different-size nails. The pool has three fountains, one in the centre, and the other two the same distance from the centre, spread evenly across the pool. There are two, probably, deliberate drainage holes, which are almost rectangular, one in the corner and the other in one side of the pool. Engraved writing is visible on five of the metal sheets; three are engraved with inscriptions, one with inscription and a signature, and one with a signature

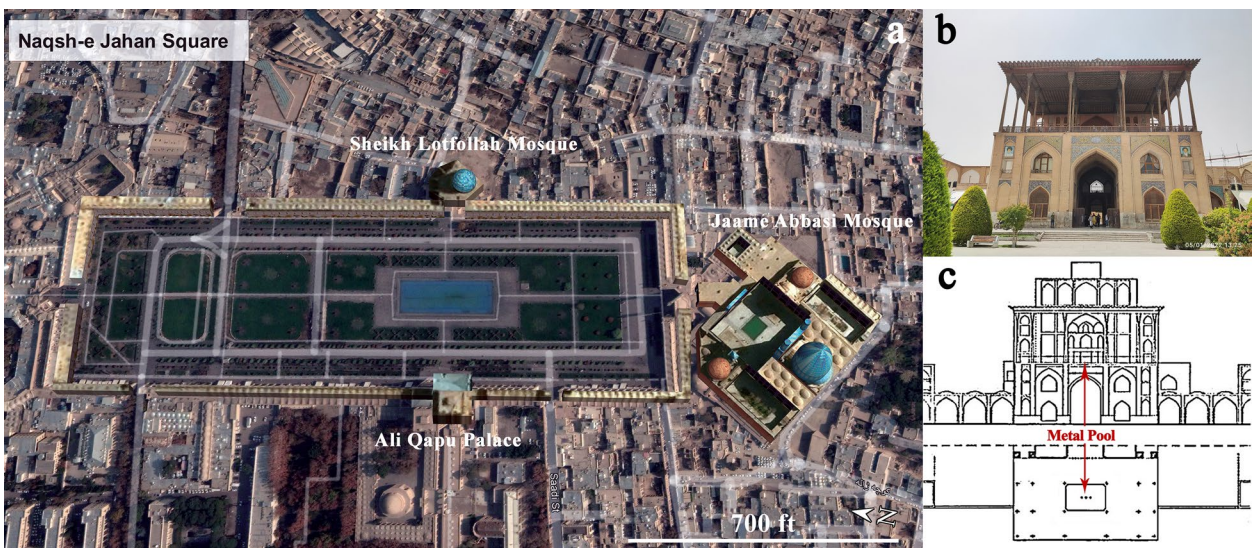

Fig. 1 **a** Aerial view of Naqsh-e Jahan Square and location of Ali Qapu Palace in the west side of the World Heritage Site (Google Earth), **b** Ali Qapu Palace from eastern view, **c** Plan of the porch of the Ali Qapu Palace showing the location of the pool on the centre of the porch [33]

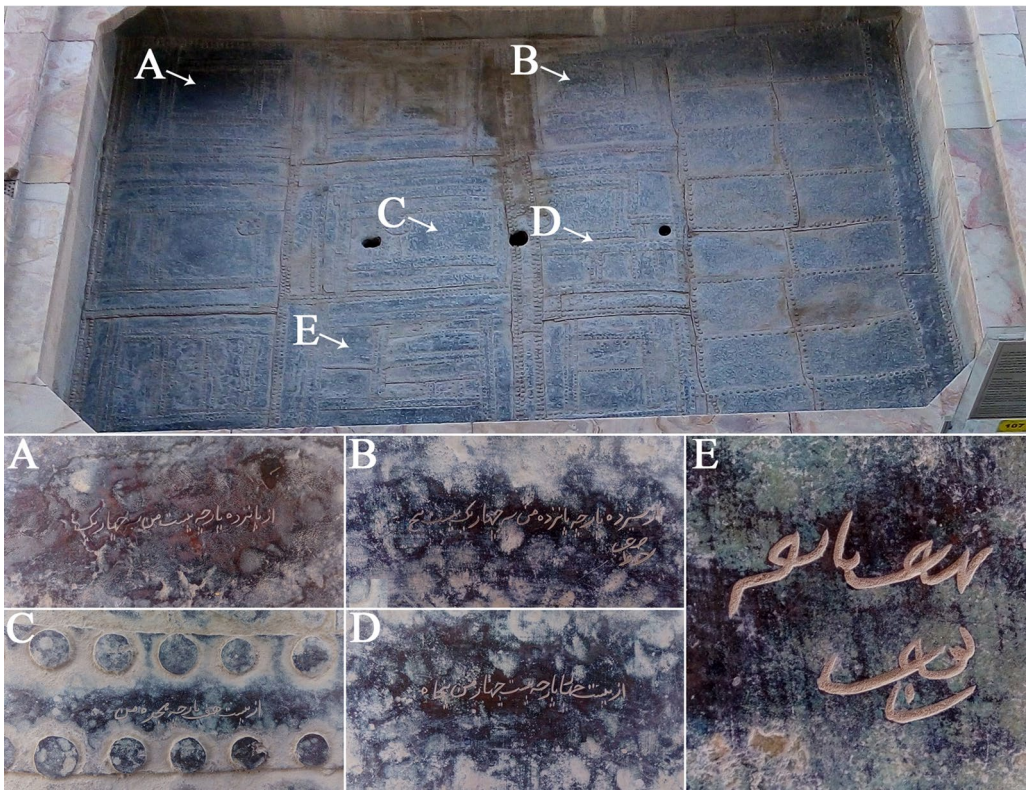

Fig. 2 The metal pool of Ali Qapu Palace, the writing boards labelled from A to E referring to the weights of the sheets. **A** "of 15 sheets 122.250 kg", **B** "of 13 sheets 92.625 kg", **C** "of 27 sheets 108 kg", **D** "of 24 sheets 144.750 kg", **E** a personal signature probably from the metalworker or copper trader

only (Fig. 2). The translation of four inscriptions are as follow while the E is a personal signature, probably from the metalworker or copper trader:

Inscription A: "of fifteen sheets 122.250 kg"
Inscription B: "of thirteen sheets 92.625 kg"
Inscription C: "of twenty-seven sheets 108 kg"
Inscription D: "of twenty-four sheets 144.750 kg"

A uniform black-brown patina covers the pool showing the long-term corrosion/oxidation in the urban environment of Isfahan. Conservators have observed the level of corrosion is increasing, hence we effort to identify the corrosion mechanism.

Materials and methods

To study the corrosion mechanisms and conservation conditions for the pool, on-site observations and laboratory analysis of collected samples were undertaken. Firstly, the metal corrosion on the sheets was observed in-situ using a digital portable stereomicroscope. Then, five samples from different parts of the pool were collected; two samples were cut from the edges of the floor and wall sheets (AQ-01 and AQ-02), a sample from a nail was taken from floor (AQ-03), and two samples were collected from the corrosion layers of the sheet surface (AQ-04 and AQ-05). Details of the samples are provided, and the sampling locations are shown in Table 1 and Fig. 3.

Three metal samples (AQ-01, AQ-02 and AQ-03) were cut into two parts. Corrosion layers were removed from one part of each sample by dissolution in aqua regia, and before the alloy composition was measured by inductively coupled plasma emission spectroscopy (ICP-OES) using an Optima 7300 DV system. The second part each sample were mounted in two-part epoxy resin (resin and hardener), then ground with abrasive paper and finally polished using diamond paste (3 and 1 microns). The polished cross sections were observed by scanning electron microscopy and optical microscopy.

The metallographic cross-sections were examined optically before and after etching using an MR-11 metallographic microscope (Ogawa Seiki company). An aqueous iron (III) chloride etchant was used to observe the microstructure of two samples of metal sheets, and a glacial acetic acid was used to etch the nail sample [34].

The SEM–EDS analyses and observations were performed on the cross sections under high vacuum using an FESEM instrument model MIRA3 field emission scanning electron microscope manufactured by

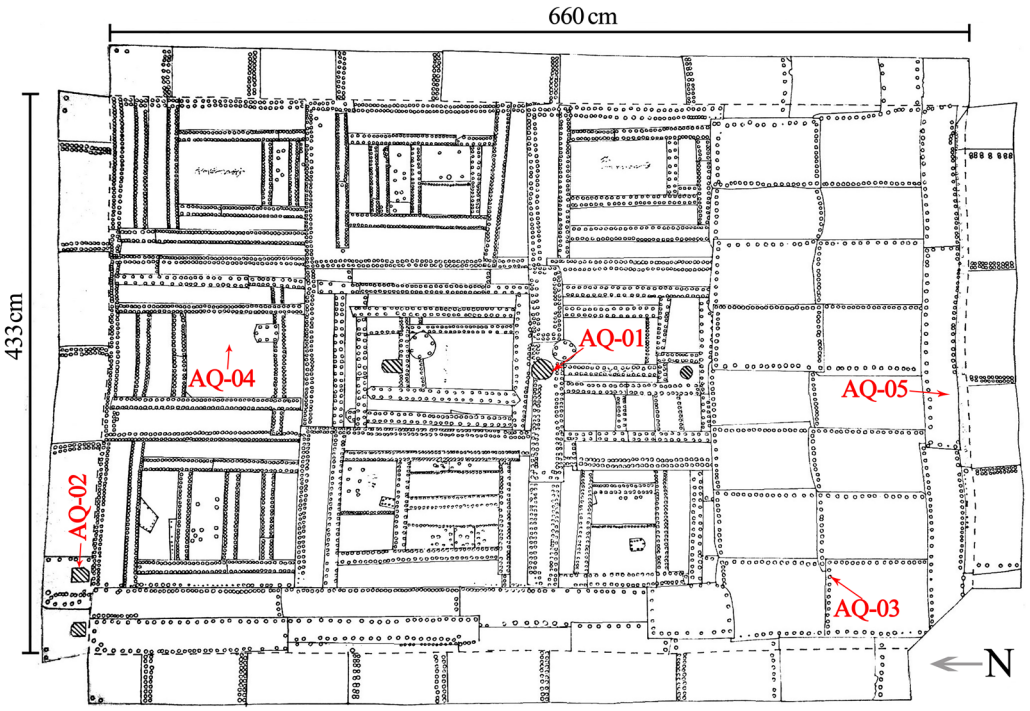

Fig. 3 Technical drawing and details of the metal sheets of the pool of the Ali Qapu Palace and marked places of sampling for analytical works

Table 1 Characteristics of five samples collected from the metal pool of the Ali Qapu Palace, including the samples' type and place of sampling

Sample	Sample's type	Place of sampling
AQ-01	Metal sheet	Edge of a metal sheet in the floor of the pool
AQ-02	Metal sheet	Edge of a metal sheet in the side wall of the pool
AQ-03	Metal nail	Edge of a metal nail in the sheet from the floor
AQ-04	Corrosion products	Corrosion layer in the floor of the pool
AQ-05	Corrosion products	Corrosion layer in the side wall of the pool

TESCAN, with a backscattered electron detector (BSE) and an energy dispersive X-ray spectrometer (EDS) (RONTEC, Germany and QUANTAX (QX2)). X-ray analysis was conducted with an accelerating voltage of 15 kV in high vacuum, with a beam size of 500–700 nm and probe current of 200–600 pA. The samples were inserted into the instrument and examined without any preparatory procedure, such as carbon or gold coating.

Two powder samples of corrosion products (AQ-04 and AQ-05) were analysed by X-ray diffraction method with an X-ray diffractometer model D8 ADVANCE manufactured by the Bruker AXS Company to detect the phase composition of the corrosion layers on the surface of the nail and metal sheets.

Results

Microscopic images

Low-magnification microscopic images (Fig. 4) show that the entire surface of the metal sheets of the Ali Qapu pool has been covered almost evenly with a black-brown smooth patina. In some parts, the corrosion products are observable in the form of light and dark green powders accompanied with a large mass of soil contaminations. Despite the patina, the metallic constituent can be observed in some of these sheets; earth-coloured pollen is scattered and accumulated in powder form, as shown in Fig. 4.

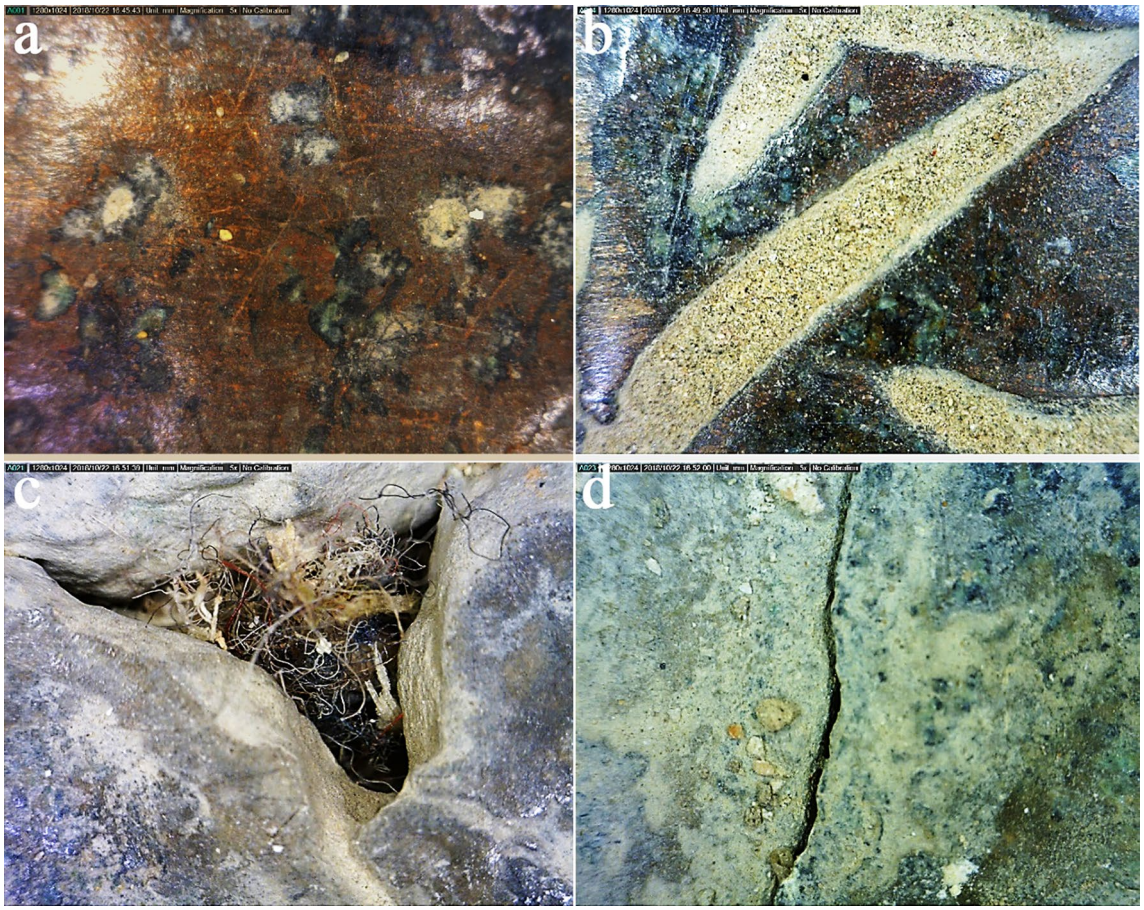

Fig. 4 Low-magnification stereomicroscopic images from the surface details of the metal sheets, magnification 10x; a) the black-brown smooth patina; b) the metallic constituent visible in the inscription parts; c) the mass of contaminations; d) the green corrosion layer and a large crack in the structure of one metal sheet.

ICP-OES analysis

The results of ICP-OES analysis are provided in Table 2. The results show leaded copper has been used in the two samples of metal sheets used for the construction of pool. The main elements in all the samples are copper and lead, 98 and 1.5 wt.% respectively, and other elements were detected in trace amounts such as Sn, Ni, Al, Fe, K, Na, As and Sb.

The results of the alloy composition analysis of a nail (AQ-03) from the pool is also presented in Table 2. It shows that the main constituent is lead for this nail and its purity is 94 wt.% and bismuth is detected as another significant constituent as 3.9 wt.%. Other elements were detected in trace amounts such as Cu, Sn, Al, Si, Fe, As, Zn and Ag.

Metallography

The unetched cross section of the samples were examined using optical microscopy and SEM–EDS. The microscopic observation of the copper sheets revealed the existence of very small holes on the microstructure of samples and the presence of a number of grey phases (Fig. 5). A large crack observed at the surface in the

Table 2 Results of the ICP-OES analysis of the metal samples from the pool (wt.%)

	Cu	Pb	Sn	Ca	Ni	Al	Si	Bi	Fe	K	Na	As	Zn	Sb	Ag
AQ-01	98	1.3	0.05	0.02	0.03	–	–	–	–	0.01	0.15	–	–	–	–
AQ-02	98	1.5	0.08	0.09	0.02	0.01	–	–	0.01	–	0.08	0.01	–	0.01	–
AQ-03	0.41	94	0.14	–	–	0.15	0.32	3.9	0.13	–	–	0.22	0.41	–	0.39

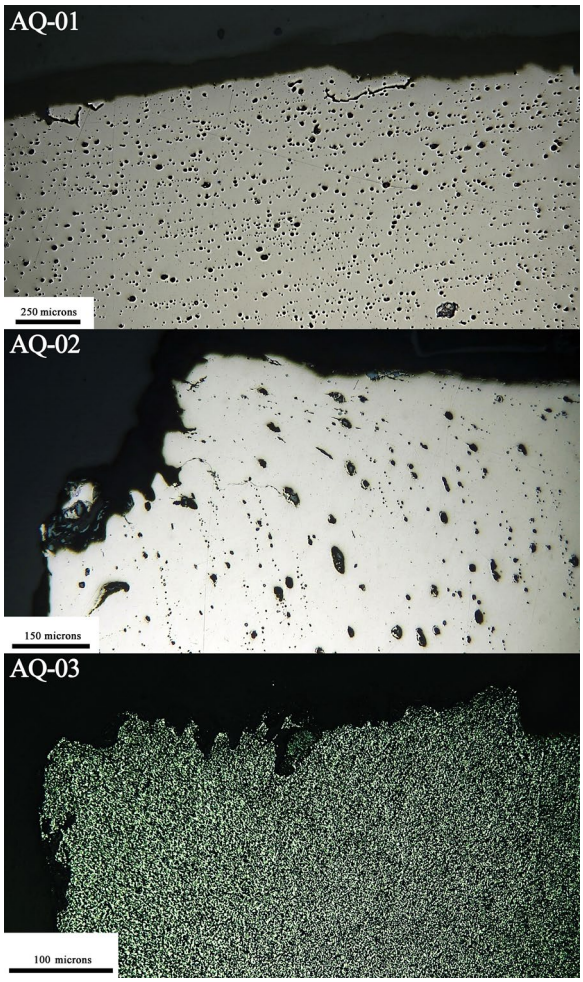

Fig. 5 Metallographic images of metal samples (optical microscopy micrograph) before etching. Microstructure of sample AQ-01 and AQ-02 includes numerous holes

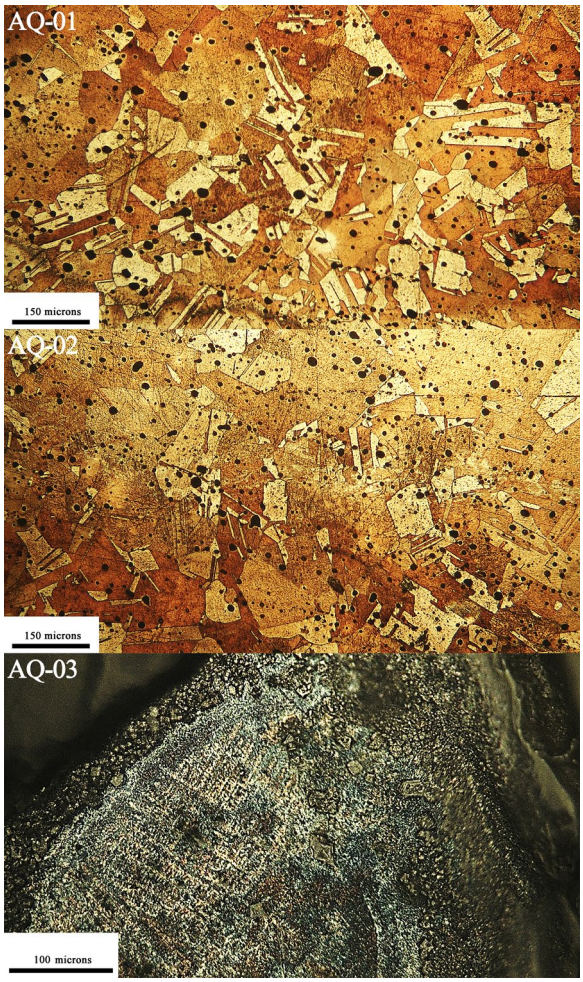

Fig. 6 The etched microstructure of the metal samples, including the worked and annealed grains with twin lines indicating that the copper sheets are shaped by cycles of the thermo-mechanical operation and the dendritic structure showing that the metal nail formed by casting

section of sample AQ-01 and smaller cracks along its length can be seen. The cracks in this work were probably due to the pressure and fatigue caused by continuous mechanical work during manufacturing the sheets.

The microscopic image before the etching of the microstructure of the sample AQ-03 shows the homogeneous structure of the material. The grain size is very small, and the distribution of the particles has formed a uniform microstructure (Fig. 5).

Images of the microstructure of the etched cross section in the two copper samples (AQ-01 and AQ-02) show the presence of equi-axed grains with twin bands. It indicates that a thermo-mechanical operation was performed on cast metal to make these copper sheets (Fig. 6). This means that copper sheets are formed by cycles of cold-working and annealing or hot-working processes. Straight twin bands and absence of strain lines shows that that annealing was used to remove stresses caused by cold-working on the metal sheets [34, 35].

The etched microstructure of sample AQ-03 shows that the grain size is very small and impurities, as grey inclusions, are scattered in microstructure (Fig. 6). A dendritic structure is visible in the entire matrix, caused by casting to form this nail [34]. The presence of worked grains and their placement is mostly at the surface of the sample, indicates some mechanical operation after the casting.

SEM–EDS analysis of phases

The results obtained from the SEM-BSE images and EDS semi-quantitative analysis of the cross sections are presented in Fig. 7 and Table 3. Two samples, AQ-01 and AQ-02, have dark grey phases (points A) which

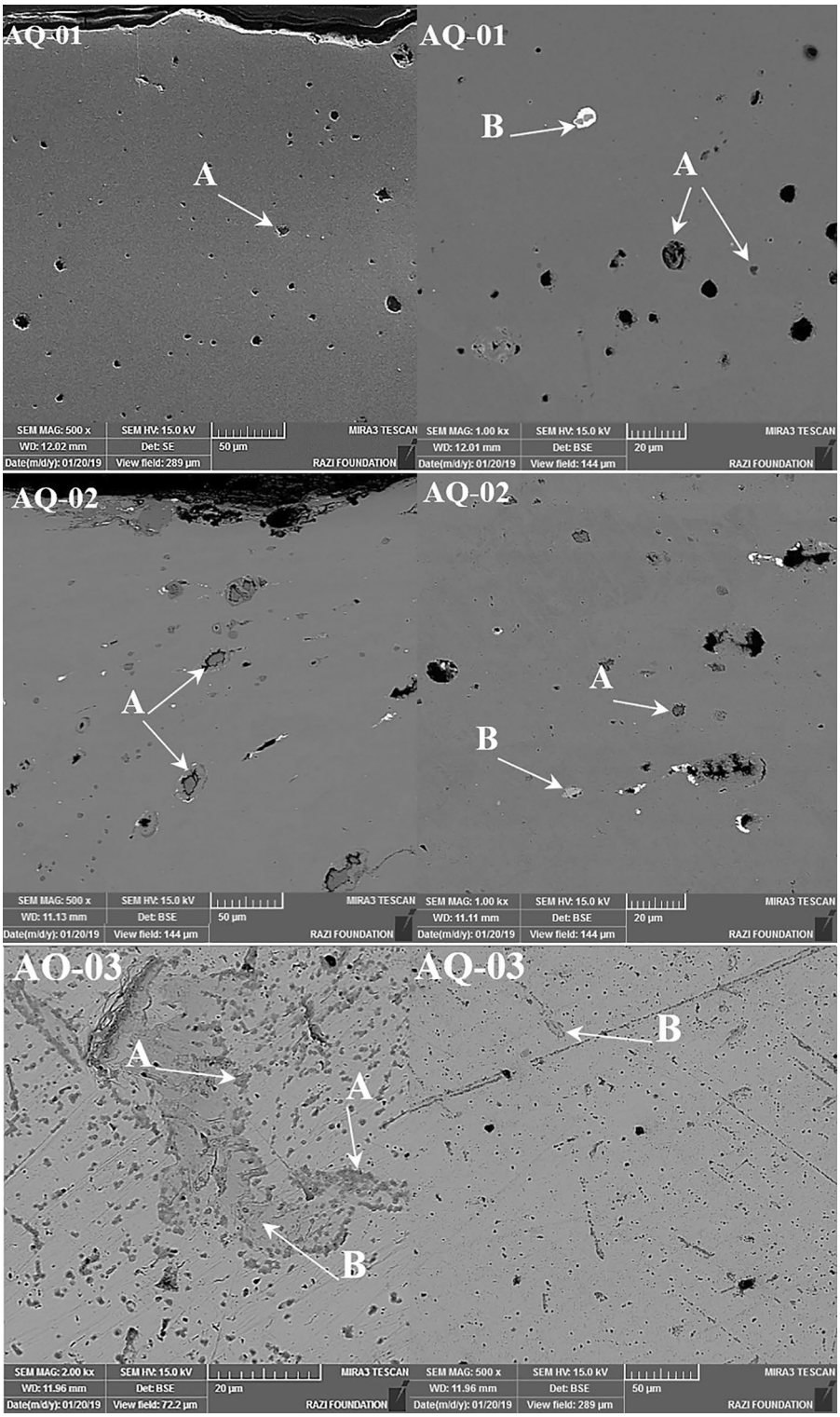

Fig. 7 SEM-BSE micrograph of samples AQ-01, AQ-02 and AQ-03 showing the inclusions scattered in the microstructure

Table 3 Results of SEM–EDS analysis of some inclusions presence in the microstructure of AQ-01 and AQ-02 samples (wt.%)

		Cu	O	Pb	As	Sn	Sb	Ag	C	Al	S	Cl	Fe	Zn	Bi
AQ-01	A	90.17	5.6	–	–	0.26	0.42	0.84	–	0.09	1.04	0.06	0.23	0.81	0.48
	A	66.25	23.02	4.13	0.61	2.00	–	–	–	0.30	–	–	0.48	2.11	1.10
	A	72.42	13.32	–	–	0.16	0.24	0.13	12.21	–	–	0.03	0.29	1.01	0.19
	B	28.91	8.79	43.38	–	5.86	–	–	8.79	–	–	–	0.38	1.25	2.64
AQ-02	A	82.26	14.74	–	–	0.24	0.35	0.23		–	1.01	–	0.31	0.86	–
	A	79.36	18.31	0.71	–	0.26	0.20	0.14	–	–	–	0.12	0.25	0.65	–
	B	34.41	7.37	40.27	–	3.24	10.41	0.00	–	–	–	–	0.20	1.19	2.91
	B	11.14	20.90	58.63	0.75	2.89	–	–	–	0.30	–	0.24	0.66	2.68	1.81

include the main elements of copper between 90.17 and 66.25 and oxygen between 23.02 and 5.6 wt.%. The presence of oxygen in the samples indicates that there are copper oxide inclusions.

Interestingly, lead-rich phases (40.27 to 58.63 wt.%) are observable as bright areas (points B) in the SEM-BSE images of both copper samples. This is because lead is immiscible in copper, so when these elements are in a molten state and are cooled, lead, which has a lower melting point (327.5 ℃), forms globules on the border of copper grains, which has a higher melting point (1084.5 ℃) [34]. It is possible that the exact amount of lead in the samples is higher than the amount detected by the semi-quantitative EDS technique. Despite the varied amount of lead globules in the microstructure of samples and lead amount in the entire composition of the sheets, it can be denoted that this element may have been present in the original copper ore from and was not added to copper for alloying purposes [36]. Given the results, it is worth noting that in addition to copper as the main element in the production of the sheets, other elements such as Pb, As, Sn, Sb, C, Al, Fe have also contributed to the creation of these sheets, and originate from the copper ores which were used to produce copper sheets.

The results obtained from the SEM-BSE images and EDS semi-quantitative analysis of the sample AQ-03 are presented in Fig. 7 and Table 4. In the dark spots (A) and bright spots (B), the main composition is lead and its amount varies between 93.33 and 88.59 wt.%. Oxygen was detected between 6.64 and 1.26 wt.%. The presence of oxygen in the samples indicates that there are also oxide inclusions. Bismuth is also present in considerable amounts. Other elements were detected in minor/trace amounts in the sample (Table 4).

Corrosion stratigraphy and analysis

To identify the corrosion layers of the copper samples (AQ-01, AQ-02), the cross sections were studied by optical microscopy before etching. The results showed that the main surface film consists of two distinct layers, namely the internal and external corrosion layer according to the original surface (OS) (Fig. 8). The internal corrosion layer (I) is red, formed within the metal structure, and is a distinct, dense layer of altered metal products formed below the OS. The external layer (II) is formed over the OS. This external corrosion layer consists of pale green corrosion products mixed with some small particles of pollutants.

The external and internal corrosion layers were analysed by SEM–EDS (Fig. 9 and Table 5). The results showed that copper and oxygen are the main constituent elements in all the corrosion layers of the copper sheets. The amount of copper decreases from the internal layer (I) to the external one (II). Other elements such as sulphur, aluminium, iron, and zinc are present in small amounts in the chemical composition of some layers which may have originated from environmental contaminations or original ore. The amount of chlorine varies

Table 4 Results of SEM–EDS analysis of inclusions in the microstructure of sample AQ-03 (wt.%)

Sample		Pb	O	Bi	S	Cu	As	Sn	Sb	Ag	Al	Si	Fe	Zn
AQ-03	A	88.59	1.4	3.11	4.90	0.39	0.32	0.25	–	0.23	0.14	0.29	0.21	0.53
	A	89.40	6.64	1.79	–	0.38	0.08	0.16	0.15	0.55	0.04	0.17	0.19	0.45
	B	93.33	1.26	2.59	–	0.29	0.44	–	0.18	0.78	0.20	0.35	0.21	0.37
	B	90.87	3.73	2.60	–	0.15	0.47	0.17	0.26	0.79	0.20	0.30	0.13	0.33

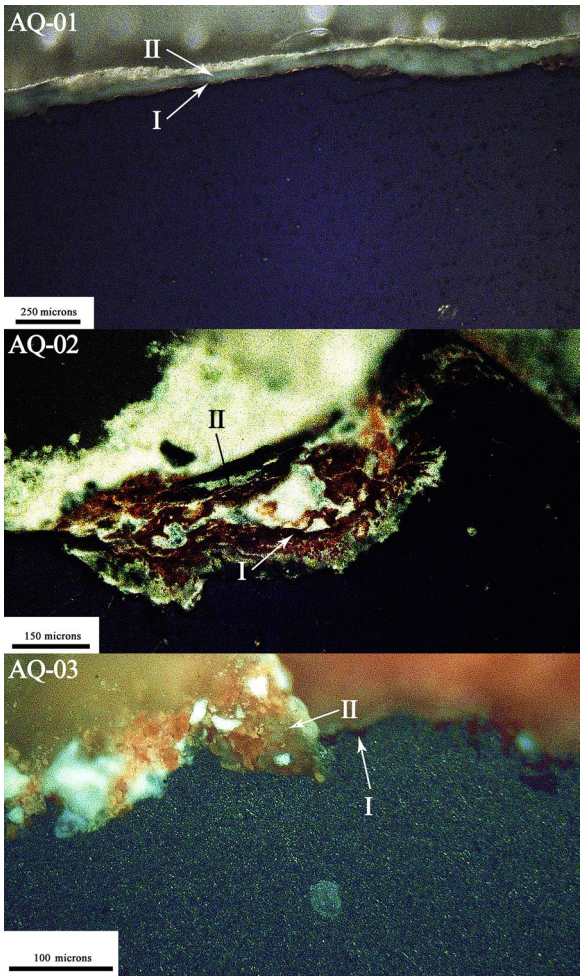

Fig. 8 Microscopic images (dark-field) of corrosion layers of metal samples showing that they consist of two distinguishable layers (I and II) on the surface of the metal sheets and the nail

between 0.28% and 9.31% and is different in the external and internal layers.

Due to the general appearance of the surface exposed to pollutants from the urban environment, layers of corrosion products have formed on the surface of the effect. Assuming that this remains in a balanced environment, this corrosion will not change [37]. The current condition of the samples is such that the border between the main metal or the main surface that defines the initial shape of the metal is completely clear and it is possible to distinguish it from the corrosion layers formed outside and inside the structure of the samples.

In the cross section of the lead sample (AQ-03), it is observable that much of the metal structure of the sample remains untouched and the limit of the original surface is clearly observable (Fig. 8). A very thin red to orange internal layer (I) is formed inside the metal structure, while the external corrosion layer (II) is white.

SEM–EDS analysis was performed to identify the corrosion layers of the AQ-03 sample (Fig. 9 and Table 6). The results showed that lead and oxygen are the main constituent elements. The amount of lead decreases from the internal layer (I) to the external layer (II). The amount of oxygen in the two external and internal layers is significant (ca. 27 and 9 wt.% respectively). Chlorine (0.37%) has only been detected in external layers. Sulphur, silicon, aluminium, and iron are also present in small amounts in the chemical composition of both layers, which may have originated from environmental pollutants.

Mineralogy of corrosion layers

To identify the mineralogy of the corrosion products, two powder samples were taken from the corrosion layers formed in different areas of the copper sheets and were analysed using XRD. The results showed that different phases were formed on the copper sheets (Fig. 10). Cuprite (Cu_2O) as well as atacamite and paratacamite ($Cu_2(OH)_3Cl$) were identified as corrosion products in the two samples. Cuprite or cuprous oxide is the most common corrosion product in different environments, such as atmosphere or soil [1, 38, 39]. Its colour is usually dark brown to dark red, orange or yellow. In many copper alloy artefacts, the main composition of patina is cuprite along with other copper (II) compounds and it creates a protective coating on the surface of the object and slows the rate of corrosion [1, 40]. The two main isomers of copper trihydroxychlorides; atacamite and paratacamite, are the main corrosion products associated with 'bronze disease' of copper alloy objects [41, 42]. They appear as powdery pale green products in copper alloy objects buried in soil or exposed to chlorine-rich seawater. Copper is detected in the corrosion layers, indicating that some metallic copper is sampled from the corrosion layers during scraping the corrosion samples. Other phases identified in the XRD analysis include compounds commonly found in soil consisting of calcite, quartz, and gypsum. This shows that the external corrosion layer is associated with particulate matters deposited on the surface of the pool.

Taking into consideration the data obtained from the analysis of the corrosion layers and the microscopic and chemical analysis of the corrosion layer of the copper sheets, it can be concluded that copper content is decreased in the internal patina in comparison with the sound metal showing that corrosion mechanism in the pool is the dissolution of copper. This has been amplified by the reaction of dissolved copper with chlorine

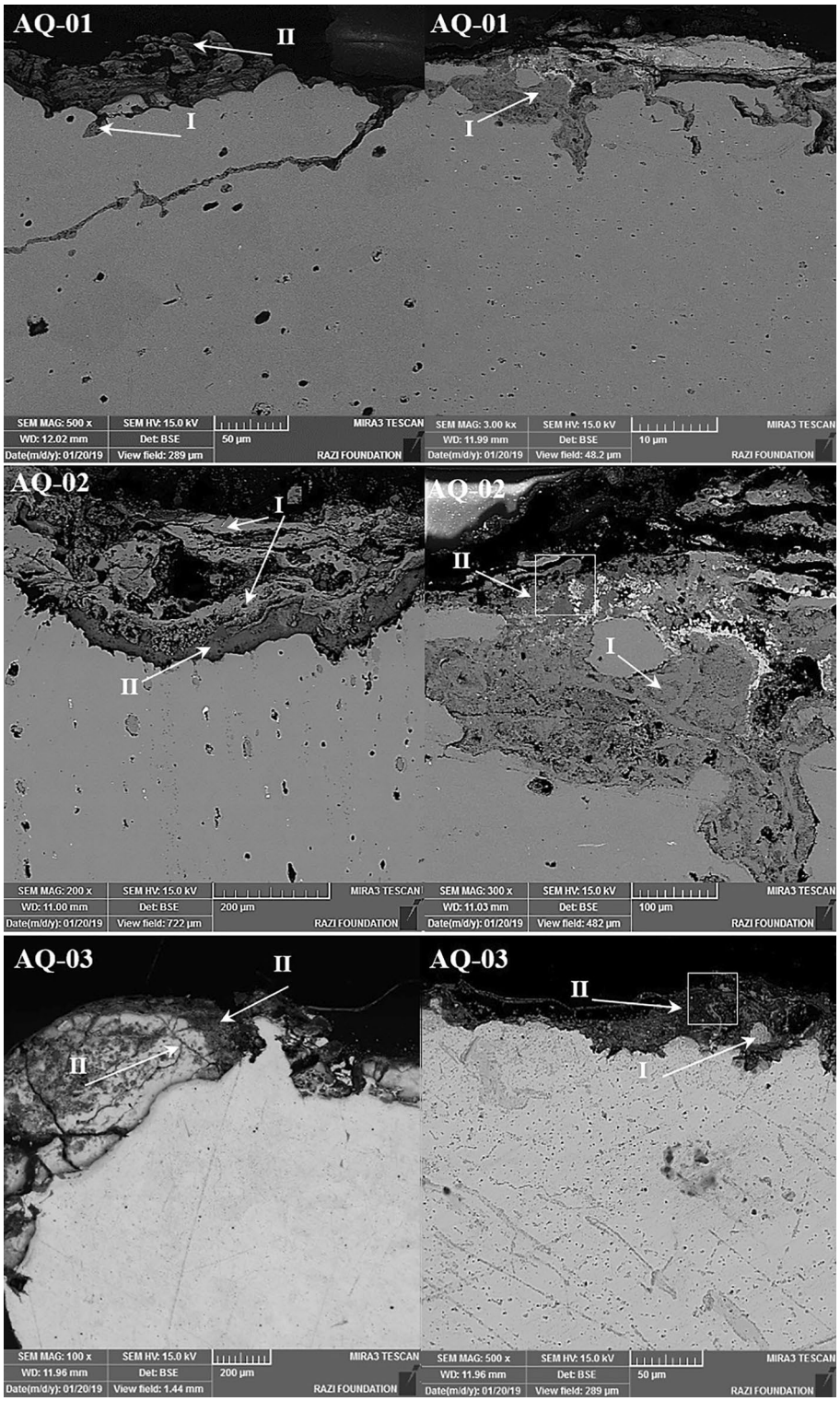

Fig. 9 SEM-BSE micrograph of corrosion layers in metal samples; two internal and external layers (layers I and II) are visible

Table 5 SEM–EDS analysis results of different internal (I) and external (II) corrosion layers of two copper samples (wt.%)

Sample		Cu	O	Cl	Pb	As	Sn	Sb	Ag	S	Fe	Al	Zn	Bi
AQ-01	I	88.38	7.31	0.13	–	0.42	0.55	0.58	0.37	0.19	0.42	0.35	0.81	0.49
	I	68.95	21.41	0.28	1.9	0.61	0.74	1.43	0.88	0.17	0.79	0.23	2.64	–
	II	64.25	22.98	1.52	–	0.53	5.65	0.32	0.41	1.36	0.37	–	1.97	–
AQ-02	I	80.01	12.06	1.04	–	–	5.04	0.21	0.14	–	0.29	–	1.21	–
	I	80.01	16.76	0.1	–	–	1.95	–	0.24	–	0.2	–	0.74	–
	I	69.32	18.18	9.31	–	–	0.41	0.79	0.43	0.46	0.29	0.12	0.69	–
	II	34.54	31.19	0.28	1.61	0.59	29.4	–	0.36	–	0.47	0.75	0.81	–
	II	26.21	2.72	0.33	–	0.33	67.98	–	0.58	0.18	0.29		0.53	0.85

Table 6 SEM–EDS analysis results of the from different internal (I) and external (II) corrosion layers of athe lead nail (wt.%)

Sample		Pb	Cu	O	Cl	As	Sn	Sb	Ag	Si	S	Fe	Al	Zn	Bi
AQ-03	I	85.82	0.50	9.62	–	–	–	0.97	0.43	0.17	–	0.14	0.04	0.77	1.54
	I	79.69	1.96	8.50	–	–	–	2.58	–	2.25	2.06	1.15	–	1.81	–
	II	51.01	0.54	27.84	0.27	8.11	–	3.56	0.20	5.42	0.43	1.09	0.05	0.34	1.14
	II	40.06	0.44	26.53	0.37	10.31	0.43	4.76	0.60	10.42	1.43	0.29	0.82	0.64	2.90

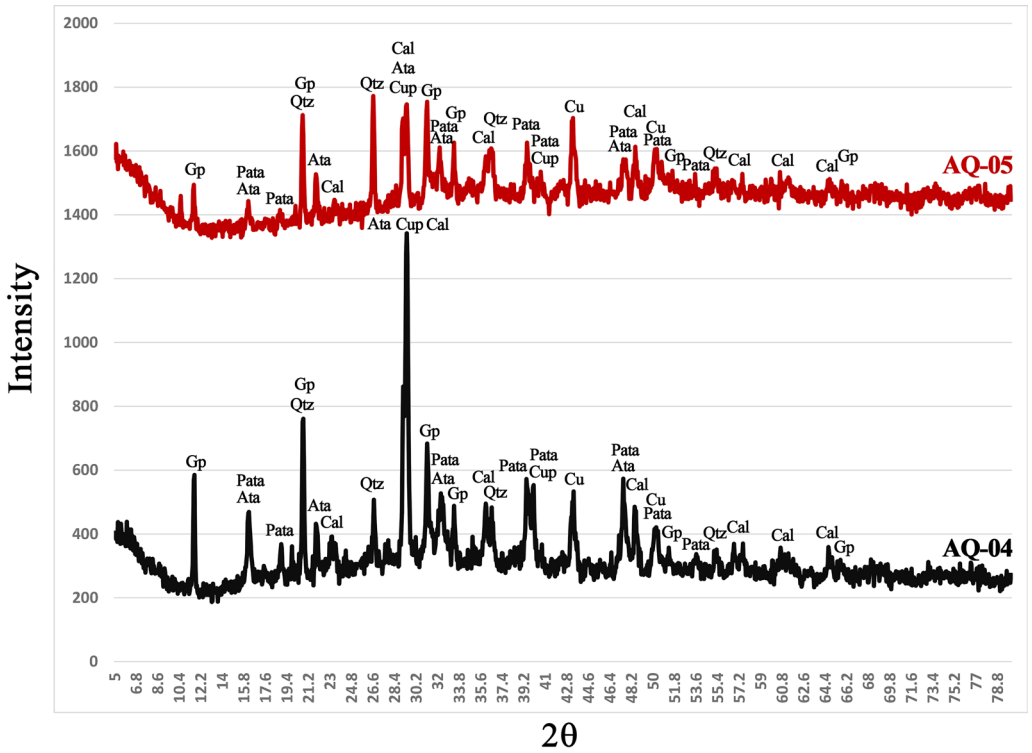

Fig. 10 X-ray diffractogram of samples AQ-04 and AQ-05 showing presence of different types of copper corrosion products and soil contaminations in the corrosion layers of the copper sheets . *Cu* copper, *Cup* cuprite, *Ata* atacamite, *Pata* paratacamite, *Qtz* quartz, *Cal* calcite, *Gp* gypsum

and re-deposition of copper trihydroxychlorides on top of the original surface.

Discussion

Corrosion mechanism of the pool

Isfahan is one of the largest industrial cities in Iran and its air contains CO_2, CO, dust, O_3, N_2, NH_3, NO_2, SH_2, formaldehyde, lead as well as different particulate matters (PM) [43, 44]. The results indicate the corrosion layers are formed due to exposure of the pool to the urban environment of Isfahan. It is important to know the composition of the environmental pollutants and the degree of climate change to determine the extent of metal corrosion in the open air. Meteorological characteristics also affect air pollution factors that cause metal corrosion. Temperature affects the corrosion of metals which are located outdoors. As the temperature rises, the rate of corrosion increases. The pool is exposed to sunlight and a layer of cuprite is formed in the presence of oxygen. This layer is homogenous and self-healing and acts as a barrier to the metal against subsequent corrosive attacks [45].

The severity and mechanism of the corrosion that has formed in the copper pool due to its exposure to the environment occurs in the first stage of the direct reaction product of copper with the oxygen in the air. This product is a result of the simple mechanism of copper oxidation to form cuprite and is observable as the internal patina. With the transfer of electrons from Cu^{1+} to Cu^{2+}, ion conduction occurs in this layer and copper migration occurs between the surface layers and oxidation occurs. Furthermore, the dissolution of copper causes the formation of copper ions [46, 47]. The following equations may be the mechanism of corrosion that occurred in the l copper sheets:

$$4Cu + O_2 \rightarrow 2Cu_2O$$

$$2Cu \rightarrow 2Cu^{2+} + 4e^-$$

Moisture is a key factor that hydrolyses monovalent copper chloride (nantokite) and creates hydrochloric acid in the presence of chloride ions, leading to formation of basic copper chlorides (atacamite and paratacamite) which is pale green in colour and has a powdery texture. Since the initial hydrolysis is a reversible reaction, unless its progress is prevented, metal corrosion will continue and increase. Fig. 11a shows the maximum and minimum average temperature from 2000 to 2019 in the city of Isfahan and Fig. 11b shows that relative humidity (RH) in the Isfahan province from 2000 to 2019 decreased in the colder months. Hence, the lowest relative humidity occurs in July and the highest relative humidity occurs in December. There has been a decrease in relative humidity over the last two decades. In a situation where dry and wet corrosion alternates or insoluble corrosion products are formed on the surface of the metal, this event becomes metal again by absorbing moisture in the dry cycle and rewetting and increases the rate of corrosion. The formation of the patina on copper are examples of atmospheric wet or dry corrosion.

When copper ions react with chloride, it turns into copper chloride (nantokite) and changes to one of the copper trihydroxychlorides in the presence of high relative humidity and oxygen. This compound forms isomers such as atacamite, paratacamite and botallackite [1]:

$$2Cu^+ + 2Cl^- \rightarrow 2CuCl$$

$$2CuCl + H_2O \rightarrow Cu_2O + 2H^+ + 2Cl^-$$

$$4CuCl + O_2 + 4H_2O \rightarrow 2Cu_2(OH)_3Cl + 2H^+ + 2Cl^-$$

$$6CuCl + 1_{1/2}O_2 + 3H_2O \rightarrow 2Cu_2(OH)_3Cl + 2Cu^{2+} + 4Cl^-$$

The presence of sulphur dioxide in the open air accelerates the corrosion of metals, although the initial reactions of copper are quite complex and depend on the relative humidity and concentration of sulphur dioxide. For example, sulphur compounds that are not oxidized may react with the metal surface and produce sulphurs, some of which are oxidized to sulphates and accelerate the rate of corrosion. Sulphur compounds can be obtained in aerosols and particles. Also, sulphur dioxide is absorbed by the surfaces of particles, including salts and metal oxides in the air masses along with dust, and is placed on the surface and turns into H_2SO_4.

The following equation shows the change in copper sulphates and transformation to copper trihydroxychlorides at the presence of chloride ions and low concentrations of SO_2 [48]:

$$Cu_4(OH)_6SO_4 + 2Cl^- \xrightarrow{H_2O} 2Cu_2(OH)_3Cl + SO_4^{2-}$$

The corrosion layers formed in the copper sheets of the pool are comparable with the corrosion layers observed in the metal dome of Hafez's tomb in Shiraz, another metropolis in southern Iran [13] where an external corrosion layer including basic copper chlorides is present, and the internal corrosion layer also contains a very thin dark layer of cuprite with visible cracks. In fact, it

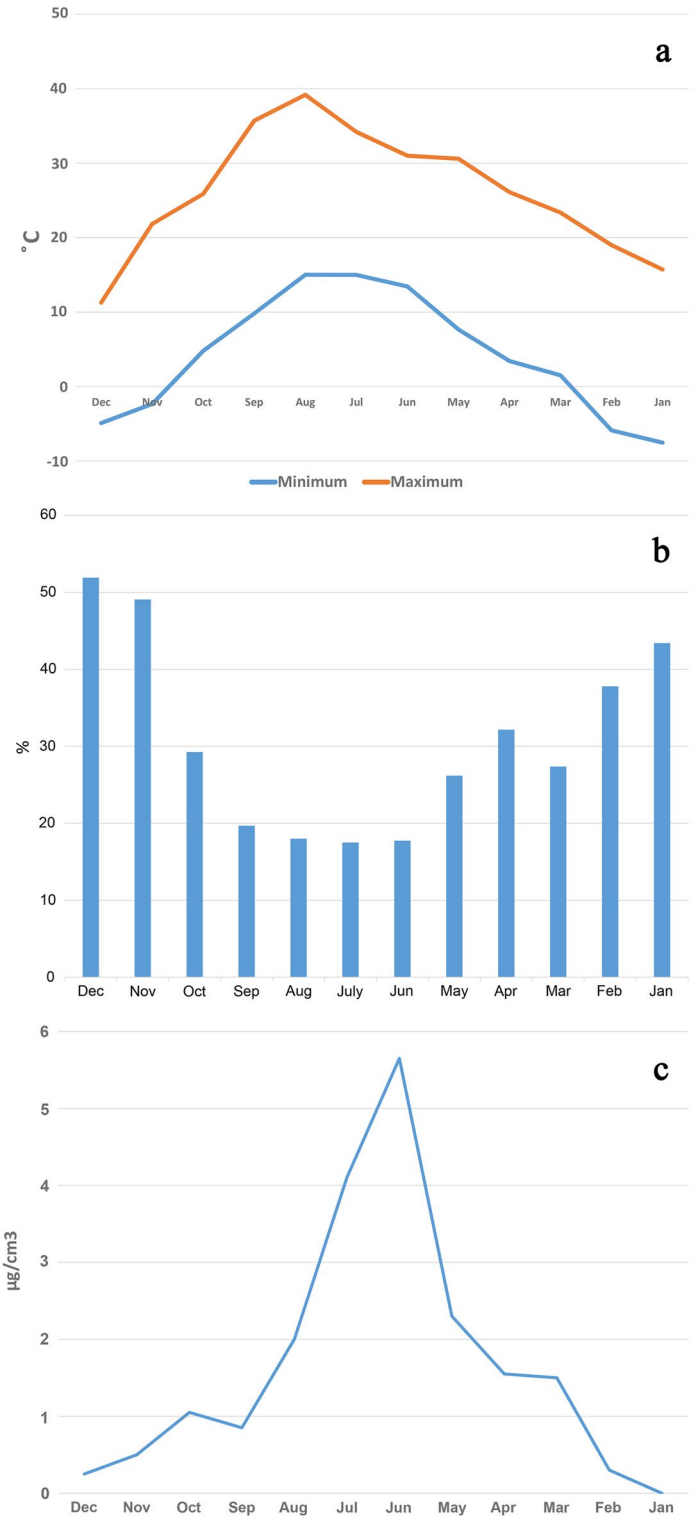

Fig. 11 **a** Average minimum and maximum temperature of Isfahan; **b** Graph of the average relative humidity of Isfahan; **c** Average of particulate matters in the air of Isfahan during 20 years (2000-2019)

shows that the corrosion mechanism occurred in both monuments is similar and influenced with particulate matters contamination.

For the lead nail, the corrosion mechanism begins when lead oxide forms on the surface. In response to carbon dioxide in the air, the lead oxide is then converted to plumbonacrite ($Pb_5O(OH)_2(CO_3)_3$) and hydrocerussite ($Pb_3O(OH)_2(CO_3)_2$) [49, 50].

In atmospheres like Isfahan's which contain sulphur oxide from industrial pollution, the order of the formation of lead corrosion products (patina) is lead oxide—lead carbonate—natural lead carbonate—natural lead sulphide—natural lead sulphate [50, 52]. Lead reacts to gases in the atmosphere such as NO_x, SO_2, CO_2 and vapours of carboxylic acids [51, 52]. Outdoor lead corrosion produces anglesite ($PbSO_4$) or cerussite ($PbCO_3$) [53]. However, we did not observed these corrosion products.

Finally, Isfahan is known to experience significant dust storms [54–56] which may have contributed to the observed corrosion. Dust storms have a detrimental effect on metal surfaces because the dust has the ability to absorb moisture and residual acids and keeping the corrosive layer in contact with the metal surface. With the seasonal investigation of the phenomenon of dust as one of the effective factors in connection with metalworks placed in the outdoor environment, for Isfahan station in the statistical period of 2000–2019, as shown in Fig. 11c. it indicates that the highest concentration of particulate matters in spring due to the increase in daylight hours, surface heating and environmental instability, as well as human factors [57, 58]. Dust storms have a detrimental effect on metal surfaces and cause corrosion because dust has the ability to hold moisture and residual acids and therefore dust particles damage the metal by sticking to the surface and absorbing water.

As an instance, study of effect of environmental conditions and corrosive factors on the corrosion and deterioration of different materials including copper alloys in Athens, Greece, shows interesting aspects that could be comparative with this study. In one study, in the frame of the European project, entitled MULTI-ASSESS, specimens of structural metals (iron, copper, bronze and zinc), glass, stone and concrete materials were exposed to air pollution at a station, which was installed for this purpose on a building, located in the centre of Athens. The main purpose of this project was to determine the corrosion and soiling effects of air pollution on materials. A set of the specimens was exposed in a position that was sheltered from rain and partly from wind, and another set was exposed in unsheltered positions on the roof of the above said building. In addition, other specimens were exposed at different heights on the same building, in order to investigate for the first time, the corrosion and soiling effects on various materials as a function of height. For the determination of these effects, chemical analysis of the specimens was performed and basic parameters as the weight change, the layer thickness and the optical properties were calculated. The most water-soluble anions formed on the surface of copper and bronze specimens were sulphate and chloride [59]. In another study, in the frame of the same project, MULTI-ASSESS, to determine these effects and to develop dose–response functions appropriate for the new multi-pollutant environment. The University of Athens participated in this effort as a targeted field exposure test site. In this study, the measurements of the passive samplers, which were exposed during the same period with the samples for corrosion studies, at the Athens station, are presented. The results have shown that only 16.5% of the deposited mass was water soluble. The vertical distribution of passive particle collectors has led to the conclusion that the height of maximum deposition of each ion is different. In addition, a variation of the water-soluble mass to total deposited mass between 8 and 31% was observed including sulphates, chlorides and nitrates [60]. These copper corrosion products are formed at the surface of the metal coupons due to presence of the air pollutants and humidity at the surface of metal, leading to corrosion of copper in different contents.

The current study tried to show the effect of the modern climate change and industrialization on the cultural heritage monuments in the city of Isfahan. As mentioned above, the number of dust storm and concentration of particulates increased during the last decade in the middle east and by nature, in Isfahan [55, 61]. Application of satellite images and numerical models in the study of the sources and routes of the dusts in the Isfahan province shows the increasing this phenomenon in the region during the last decades [62]. In fact, these kinds of analytical and filed study on the effect of environmental effects and climate changes on the cultural heritage is in accordance with the Sustainable Development Goals-UN 2030 agenda, in which "take urgent action to combat climate change and its impacts" is mentioned [63]. Accordingly, the effect of climate changes is apparently observable in different aspects of our life in the recent years, and the cultural heritage monuments and objects are affected seriously due to their sensitivity and conditions after long-term decay in different environments and it was observed in different scientific studies undertaken in this field [64–67]. Consequently, these case studies could help conservators and heritage scientists to understand different aspects of climate change and air pollution on the

durability and decay mechanism in the cultural heritage monuments.

Conservation plan for the pool

As particulate matter (PM) or dust and relative humidity are the main cause of bronze disease in the Ali Qapu Palace pool, the necessary measures should be taken to clean the surface of copper sheets and remove the layer of solid contaminated pollutants. This layer is contaminated with chlorine, and in conjunction with high RH, it may cause persistent bronze disease. Also, the dust layer is formed of particulate matters and sometimes is thick and very hygroscopic [68]. Not only can this layer maintain a high humidity level on the metal sheets' surface, but its results in a dirty appearance for the pool.

Since cuprite patina has prevented copper oxidation, the use of artificial coatings on the pool surfaces is not necessary, although application of organic coatings was suggested as a protective method in recent years [69–71]. There should also be a periodic monitoring program to observe and evaluate the condition of the pool protection. The streaks of bright green corrosion products and the presence of sediments not only damage the stability of the copper sheets but also the appearance and creates many problems for the conservators to clean the surface from contaminations. Such monuments often need to be cleaned by using different cleaning methods and materials [1, 3, 72]. The purpose of cleansing should be the least possible and consistent with the aesthetic goals along with the suggestion. Finally, to protect and restore the pool, an effective maintenance program including periodic monitoring and cleaning the surface of the pool (a housekeeping plan) is required after the implementation of the protection treatment steps. Cleaning should be done periodically to prevent re-contamination of the surface of the copper sheets.

Conclusion

The metal pool of the Ali Qapu Palace in Isfahan, is exposed to the urban environment and is corroded in long-term exposure to the corrosive factors and pollutants. This study has shown that the metal sheets are low-leaded copper, which are indicative of Iranian metalworkers using traditional methods to form the sheets. The corrosion mechanism in the copper sheets showed the copper oxidation in the sheets and the formation of an internal dark layer, included cuprite as the main phase, and an external green layer consisting of copper trihydroxychlorides and very small particles of particulate matters. Furthermore, the corrosion mechanism in a lead nail showed lead oxidation. Even though the pool is situated in an urban environment, the main factors in the corrosion of this metal pool are relative humidity and particulate matters, which may include chloride ion that can lead to active corrosion or bronze disease. This corrosion event appears to be in the early stages and has not yet caused serious problems in the copper sheets. However, monitoring the conditions in terms of the amount and penetration of corrosion is essential to decide on the metal pool conservation strategy. Further studies may focus on investigating future conservation strategies for the metal pool.

Acknowledgements
The Authors are grateful to Dr. Rose King (The Metropolitan Museum of Art) for her comments and editing on the final version, Dr. Fariba Khatabakhsh and Meysam Kazemian (ICHTO Office of Isfahan Province) for their helps and support to undertake the field works and sampling.

Author contributions
MR contributed to the sampling and analytical works and interpretation of the analytical data as well as preparing the draft of the manuscript; OO contributed in the analytical works and interpretation of the analytical data as well as editing the manuscript.

Funding
Not applicable.

Availability of data and materials
The datasets used and/or analysed during the current study are available from the corresponding author on reasonable request.

Declarations

Competing interests
"The authors declare that they have no competing interests."

Received: 19 March 2023 Accepted: 18 June 2023
Published online: 28 June 2023

References

1. Scott DA. Copper and bronze in art, corrosion, colorants, conservation. Los Angeles: Getty Conservation Institute; 2002.
2. Mikhailov AA, Suloeva MN, Vasilieva EG. Environmental aspects of atmospheric corrosion. Water Air Soil Pollut. 1995;85:2673–8.
3. Knotkova D, Kreislova K. Atmospheric corrosion and conservation of copper and bronze. In: Moncmanova A, editor. Environmental deterioration of materials, wit transactions on state-of-the-art in science and engineering. Billerica: WIT press; 2007. p. 107–42.
4. Tidblad J. Atmospheric corrosion of metals in 2010–2039 and 2070–2099. Atmos Enviro. 2012;55:1–6.
5. Letardi P. Testing new coatings for outdoor bronze monuments: a methodological overview. Coatings. 2021;11:131.
6. Tidblad J. Atmospheric corrosion of metallic heritage artefacts: processes and prevention. In: Dillmann P, Watkinson D, Angelini E, Adriaens A, editors. Corrosion and conservation of cultural heritage metallic artefacts. Amsterdam: Elsevier Ltd; 2013. p. 37–52.
7. Singh JK, Paswan S, Saha D, Pandya A, Singh DDN. Role of air pollutant for deterioration of Taj Mahal by identifying corrosion products on surface of metals. Int J Environ Sci Te. 2022;19:829–38.
8. Basso E, Pozzi F, Reiley MC. The Samuel F. B. Morse statue in Central Park: scientific study and laser cleaning of a 19th-century American outdoor bronze monument. Herit Sci. 2020;8:8.
9. Källbom A, Almevik G. Maintenance of painted steel-sheet roofs on historical buildings in Sweden. Inter J Archit Herit. 2022;16:538–52.

10. Masi G, Esvan J, Josse C, Chiavari C, Bernardi E, Martini C, Bignozzi MC, Gartner N, Kosec T, Robbiola L. Characterization of typical patinas simulating bronze corrosion in outdoor conditions. Mater Chem Phys. 2017;200:308–21.
11. Di Turo F, Proietti C, Screpanti A, Fornasier MF, Cionni I, Favero G, De Marco A. Impacts of air pollution on cultural heritage corrosion at European level: what has been achieved and what are the future scenarios. Environ Pollut. 2016;218:586–94.
12. Petiti C, Toniolo L, Gulotta D, Mariani B, Goidanich S. Effects of cleaning procedures on the long-term corrosion behavior of bronze artifacts of the cultural heritage in outdoor environment. Environ Sci Pollut Res. 2020;27:13081–94.
13. Oudbashi O, Fadaei H. After eighty years: experimental study of atmospheric corrosion in the metallic dome of Hafez's tomb, Shiraz, Iran. Stud Conserv. 2019;64:208–20.
14. De la Fuente D, Simancas J, Morcillo M. Morphological study of 16-year patinas formed on copper in a wide range of atmospheric exposures. Corros Sci. 2008;50:268–85.
15. Fitzgerald KP, Nairn J, Skennerton G, Atrens A. Atmospheric corrosion of copper and the colour, structure and composition of natural patinas on copper. Corros Sci. 2006;48:2480–509.
16. Chiavari C, Bernardi E, Balbo A, Monticelli C, Raffo S, Bignozzi MC, Martini C. Atmospheric corrosion of fire-gilded bronze: corrosion and corrosion protection during accelerated ageing tests. Corros Sci. 2015;100:435–47.
17. Chang T, Herting G, Goidanich S, Amaya JS, Arenas MA, Le Bozec N, Wallinder IO. The role of Sn on the long-term atmospheric corrosion of binary Cu-Sn bronze alloys in architecture. Corros Sci. 2019;149:54–67.
18. Robbiola L, Rahmouni K, Chiavari C, Martini C, Prandstraller D, Texier A, Takenouti H, Vermaut P. New insight into the nature and properties of pale green surfaces of outdoor bronze monuments. Appl Phys A-Mater. 2008;92:161–9.
19. Chiavari C, Bernardi E, Martini C, Morselli L, Ospitali F, Robbiola L, Texier A. Predicting the corrosion behaviour of outdoor bronzes: assessment of artificially exposed and real outdoor samples. In: Mardikian P, Chemello C, Watters C, Hull P, editors. Metal 2010. South Carolina: Clemson University; 2011. p. 218–26.
20. Petitmangin A, Guillot I, Chabas A, Nowak S, Saheb M, Alfaro SC, Blanc C, Fourdrin C, Ausset P. The complex atmospheric corrosion of α/δ bronze bells in a marine environment. J Cult Herit. 2021;52:153–63.
21. Chiavari C, Rahmouni K, Takenouti H, Joiret S, Vermaut P, Robbiola L. Composition and electrochemical properties of natural patinas of outdoor bronze monuments. Electrochim Acta. 2007;52:7760–9.
22. Bernardi E, Chiavari C, Martini C, Morselli L. The atmospheric corrosion of quaternary bronzes: an evaluation of the dissolution rate of the alloying elements. Appl Phys A-Mater. 2008;92:83–9.
23. Chabas A, Fouqueau A, Attoui M, Alfaro SC, Petitmangin A, Bouilloux A, Saheb M, Coman A, Lombardo T, Grand N, Zapf P, Berardo R, Duranton M, Durand-Jolibois R, Jerome M, Pangui E, Correia JJ, Guillot I, Nowak S. Characterisation of CIME, an experimental chamber for simulating interactions between materials of the cultural heritage and the environment. Environ Sci Pollut Res. 2015;22:19170–83.
24. De Marco A, Screpanti A, Mircea M, Piersanti A, Proietti C, Fornasier MF. High resolution estimates of the corrosion risk for cultural heritage in Italy. Environ Pollut. 2017;226:260–7.
25. Masi G, Balbo A, Esvan J, Monticelli C, Avila J, Robbiola L, Chiavari C. X-ray Photoelectron Spectroscopy as a tool to investigate silane-based coatings for the protection of outdoor bronze: The role of alloying elements. Appl Surf Sci. 2018;433:468–79.
26. Lhéronde M, Bouttemy M, Mercier-Bion F, Neff D, Apchain E, Etcheberry A, Dillmann P. X-ray photoelectron spectroscopy characterization of Cu compounds for the development of organic protection treatments dedicated to heritage Cu objects preservation. Surf Inter Anal. 2020;52:1011–6.
27. Squarcialupi MC, Bernardini GP, Faso V, Atrei A, Rovida G. Characterisation by XPS of the corrosion patina formed on bronze surfaces. J Cult Herit. 2002;3:199–204.
28. Muller J, Lorang G, Leroy ER, Laik B, Guillot I. Electrochemically synthesised bronze patina: characterisation and application to the cultural heritage. Corros Eng Sci Techn. 2010;45:322–6.
29. Haneda M, Matthee R. Isfahan VII. Safavid Period, In: Yarshater E. (Ed). Encyclopaedia Iranian Online. Vol. XIII, Fasc. 6. 2006; https://www.iranicaonline.org/articles/isfahan-vii-safavid-period
30. Amin al-Raaya M. Ali Qapu palace, art treasure of, Isfahan. Isfahan: Asemannagar Publishing House; 2015.
31. Babaie S, Haug R. Isfahan X. Monuments, In: Yarshater E. (Ed.). Encyclopaedia Iranian Online. Vol. X, Fasc. 1, 2007; https://www.iranicaonline.org/articles/isfahan-x-monuments
32. Pirnia M. Iranian architectural methods. Tehran: Islamic Publishing and Art Institute Publications; 2004.
33. Galdieri E, Eṣfahān, ʿAlī Qāpū: An Architectural Survey, Istituto italiano per il Medio ed Estremo Oriente, 1979.
34. Scott DA. Metallography and microstructure of ancient and historic metals. Los Angeles: Getty Conservation Institute; 1991.
35. Scott DA, Schwab R. Metallography in archaeology and art. Springer Nature Switzerland AG: Springer Cham; 2019.
36. Oudbashi O, Hessari M. Iron Age tin bronze metallurgy at Marlik, Northern Iran: an analytical investigation. Archaeol Anthropol Sci. 2017;9:233–49.
37. Fernandes R. Study on Roman and Merovingian copper alloyed artefacts-in soil corrosion processes and recycling practices. Amsterdam: Vrije Universiteit Amsterdam; 2009.
38. Selwyn LS. Metals and corrosion: a handbook for the conservation professional. Ottawa: Canadian Conservation Institute; 2004.
39. Selwyn LS. Corrosion of metal artifacts in buried environments. In: Cramer SD, Covino BS, editors. ASM handbook, Vol. 13C, corrosion: environments and industries. Ohio: ASM International; 2006. p. 306–22.
40. Selwyn LS, Roberge PR. Corrosion of metal artifacts displayed in outdoor environments. In: Cramer SD, Covino BS, editors. ASM handbook, Vol 13C, corrosion: environments and industries. Ohio: ASM International; 2006. p. 289–305.
41. Liua W, Li M, Wu N, Liu S, Chen J. A new application of Fiber optics reflection spectroscopy (FORS): identification of "bronze disease" induced corrosion products on ancient bronzes. J Cult Herit. 2021;49:19–27.
42. Scott DA. A review of copper chlorides and related salts in bronze corrosion and as painting pigments. Stud Conserv. 2000;45:40–52.
43. Karimi H, Soffianian A, Mirghaffari N, Soltani S. Determining air pollution potential using geographic information systems and multi-criteria evaluation: a case study in Isfahan Province in Iran. Environ Process. 2016;3:229–46.
44. Hajizadeh Y, Jafari N, Fanaei F, Ghanbari R, Mohammadi A, Behnami A, Jafari A, Aghababayi M, Abdolahnejad A. Spatial patterns and temporal variations of traffic-related air pollutants and estimating its health effects in Isfahan city, Iran. J Environ Health Sci Engineer. 2021;19:781–91.
45. Leygraf C, Wallinder IO, Tidblad J, Graedel T. Atmospheric corrosion. Hoboken: Wiley; 2016.
46. Manti P, Watkinson D. Corrosion phenomena and patina on archaeological low-tin wrought bronzes: New data. J Cult Herit. 2022;55:158–70.
47. He L, Liang J, Zhao X, Jiang B. Corrosion behavior and morphological features of archeological bronze coins from Ancient China. Microchem J. 2011;99:203–12.
48. Strandberg H, Johansson L-G, Lindqvist O. The atmospheric corrosion of statue bronzes exposed to SO_2 and NO_2. Mater Corros. 1997;48:721–30.
49. Gonzalez V, Wallez G, Calligaro Th, Gourier D, Menu M. Synthesizing lead white pigments by lead corrosion: new insights into the ancient manufacturing processes. Corros Sci. 2019;146:10–7.
50. Msallamova S, Kouril M, Strachotova KC, Stoulil J, Popova K, Dvorakova P. Historical lead seals and the influence of disinfectants on the lead corrosion rate. Herit Sci. 2019;7:18.
51. Black L, Allen GC. Nature of lead Patination. Brit Corros J. 1999;34:192–7.
52. Graedel TE. Chemical mechanisms for the atmospheric corrosion of lead. J Electrochem Soc. 1994;141:922.
53. Cook AR, Smith R. Atmospheric corrosion of lead and its alloys. In: Ailor WH, editor. Atmospheric corrosion. Hoboken (New Jersey, United States): John Wiley & Sons Inc; 1982. p. 393–404.
54. Goudie A. Desert dust and human health disorders. Environ Inter. 2014;63:101–13.
55. Jafari M, Mesbahzadeh T, Masoudi R, Zehtabian G, Amouei TM. Dust storm surveying and detection using remote sensing data, wind tracing, and atmospheric thermodynamic conditions (case study: Isfahan Province, Iran). Air Qual Atmos Health. 2021;14:1301–11.

56. Rashki A, Kaskaoutis DG, Goudie AS, Kahn RA. Dryness of ephemeral lakes and consequences for dust activity: the case of the Hamoun drainage basin, southeastern Iran. Sci Tot Environ. 2013;434:552–64.
57. Rezazadeh M, Irannejad P, Shao Y. Climatology of the middle dust events. Aeol Res. 2013;10:103–9.
58. Hamidi M, Kavianpour MR, Shoa Y. Synoptic analysis of dust storms in the middle east. Asia-Pac J Atmos Sci. 2013;49:279–86.
59. Tzanis C, Varotsos C, Christodoulakis J, Tidblad J, Ferm M, Ionescu A, Lefevre R-A, Theodorakopoulou K, Kreislova K. On the corrosion and soiling effects on materials by air pollution in Athens. Greece Atmos Chem Phys. 2011;11:12039–48.
60. Tzanis C, Varotsos C, Ferm M, Christodoulakis J, Assimakopoulos MN, Efthymiou C. Nitric acid and particulate matter measurements at Athens, Greece, in connection with corrosion studies. Atmos Chem Phys. 2009;9:8309–16.
61. Rashki A, Middleton NJ, Goudie AS. Dust storms in Iran—distribution, causes, frequencies and impacts. Aeol Res. 2021;48:100655.
62. Jafari M, Zehtabian G, Ahmadi H, Mesbahzadeh T, Norouzi AA. Detection of dust storm paths using numerical models and satellite images (case study: Isfahan province). Iran J Rang Des Res. 2019;26:29–38.
63. Varotsos CA, Cracknell AP. Remote sensing letters contribution to the success of the sustainable development goals—UN 2030 agenda. Remote Sens Lett. 2020;11:715–9.
64. Orr SA, Richards J, Fatorić S. Climate change and cultural heritage: a systematic literature review (2016–2020). Hist Environ Policy Pract. 2021;12:434–77.
65. Sesana E, Gagnon AS, Ciantelli Ch, Cassar J, Hughes JJ. Climate change impacts on cultural heritage: a Literature review. Wires Clim Change. 2021;12:1–29.
66. Cassar M, Pender R. The impact of climate change on cultural heritage: evidence and response. In: Verger I, editor. ICOM committee for conservation: 14th triennial meeting. London: James & James; 2005. p. 610–6.
67. Fatorić S, Seekamp E. Are cultural heritage and resources threatened by climate change? A systematic literature review. Clim Change. 2017;142:227–54.
68. Robbiola L, Fiaud C, Pennec S. New model of outdoor bronze corrosion and its implications for conservation. ICOM Committee for Conservation tenth triennial meeting, Aug 1993, Washington DC, United States, 1993. p. 796-802
69. Masi G, Aufray M, Balbo A, Bernardi E, Bignozzi MC, Chiavari C, Esvan J, Gartner N, Grassi V, Josse C, Kosec T, Martini C, Monticelli C, Škrlep L, Sperotto W, Švara Fabjan E, Tedesco E, Zanotto F, Robbiola L. B-IMPACT project: eco-friendly and non-hazardous coatings for the protection of outdoor bronzes. IOP Conf Ser-Mat Sci. 2020;949:012097.
70. Kosec T, Škrlep L, Vara Fabjan E, Sever Škapin A, Masi G, Bernardi E, Chiavari C, Josse C, Esvan J, Robbiola L. Development of multi-component fluoropolymer based coating on simulated outdoor patina on quaternary bronze. Prog Org Coat. 2019;131:27–35.
71. Salvadori B, Cagnini A, Galeotti M, Porcinai S, Goidanich S, Vicenzo A, Celi C, Frediani P, Rosi L, Frediani M, Giuntoli G, Brambilla L, Beltrami R, Trasatti S. Traditional and innovative protective coatings for outdoor bronze: application and performance comparison. J Appl Polym Sci. 2018;135:46011.
72. Bertasa M, Korenberg C. Successes and challenges in laser cleaning metal artefacts: a review. J Cult Herit. 2022;53:100–17.

Publisher's Note